

Dissociative double ionization of CO in orthogonal two-color laser fieldsQiyong Song,¹ Peifen Lu,¹ Xiaochun Gong,¹ Qinying Ji,¹ Kang Lin,¹ Wenbin Zhang,¹ Junyang Ma,¹ Heping Zeng,¹ and Jian Wu^{1,2,*}¹*State Key Laboratory of Precision Spectroscopy, East China Normal University, Shanghai 200062, China*²*Collaborative Innovation Center of Extreme Optics, Shanxi University, Taiyuan 030006, China*

(Received 3 August 2016; revised manuscript received 4 November 2016; published 18 January 2017)

We experimentally investigate dissociative double ionization of CO by a phase-controlled orthogonal two-color (OTC) laser pulse. Directional breaking of doubly ionized CO as a function of both kinetic energy and emission direction of the nuclear fragments is observed in the polarization plane steered by the laser phase. It is attributed to the dominating sequential double ionization at the maximum strength and nonsequential double ionization at a relatively weak strength of the spatiotemporally shaped oscillating laser field pointing to various directions. Our results are interesting not only for two-dimensional control of directional bond breaking, but also strengthen our understanding of strong-field sequential and nonsequential double ionization of molecules which are spatiotemporally streaked to various directions and kinetic energies by an OTC laser pulse.

DOI: [10.1103/PhysRevA.95.013406](https://doi.org/10.1103/PhysRevA.95.013406)**I. INTRODUCTION**

For its important implications of steering chemical reactions [1,2], coherent control of directional molecular bond breaking has gotten much attention in the past decades. Carrier-envelope phase stabilized few-cycle [3–7] or two-color [8–15] ultrashort laser pulses are powerful tools to control the directional dissociative ionization of molecules. The underlying physics varies for different kinds of molecules and ionization processes. It includes the pathway interference of the dissociating nuclear wave packets of different parities in dissociative single ionization of the simplest molecule of H₂ and its isotopes [16–20]. As described by the molecular Ammosov-Delone-Krainov (MO ADK) theory [21,22] or strong-field approximation [23], the directional bond breaking of a multielectron molecule with asymmetric orbital distribution along the molecular axis, e.g., CO, is dominated by the profile of the ionizing orbital and affected by the Stark effect [24,25]. In addition to the selective ionization governed by the orbital shape of a spatially orientated molecule, it has been recently demonstrated that the laser coupling of various electronic states in the dissociation process also contributes to the directional breaking of singly ionized heteronuclear molecules [26].

Most of the examples of directional control of molecular breaking were limited to one dimension with respect to the polarization direction of the laser field [3–20]. Although two-dimensional directional dissociation was recently demonstrated for single ionization of H₂ [27,28]—the simplest two-electron molecule—no observation in multielectron molecules has been reported. Here, taking CO as a prototype, we report the observation of two-dimensional directional dissociative double ionization of a multielectron molecule by using an intense phase-controlled orthogonal two-color (OTC) laser pulse. By finely tuning the relative phase of the OTC pulse, we observed directional breaking of doubly ionized CO as a function of both kinetic energy and emission direction of the nuclear fragment. It is attributed to the sequential and non-

sequential double ionization occurring in the spatiotemporally shaped OTC pulse by laser fields pointing to various directions with different instantaneous strengths.

II. EXPERIMENTAL SETUP AND RESULTS

We performed the experimental measurements in an ultrahigh-vacuum reaction microscope setup of cold target recoil ion momentum spectroscopy (COLTRIMS) [29,30], as schematically illustrated in Fig. 1. The OTC laser pulse was produced in a collinear scheme [13] by frequency-doubling a near-infrared femtosecond laser pulse from a Ti:sapphire amplifier (25 fs, 790 nm, 10 kHz) in a 150- μ m-thick β -barium borate (BBO) crystal. The time lag between the fundamental-wave (FW, polarized along the y axis) and the second-harmonic (SH, polarized along the z axis) fields was compensated using a birefringent α -BBO crystal. The relative phase ϕ_L between the FW and SH waves of the OTC pulse is continuously varied by scanning the inset of a pair of fused-silica wedges. The produced OTC pulses were afterwards focused onto the supersonic molecular beam by a concave reflection mirror ($f = 75$ mm) inside the apparatus. The supersonic molecular beam was produced by coexpanding a mixture of 10% CO and 90% He through a 30- μ m nozzle under a driving pressure of 1.0 bar. The laser intensities of FW and SH fields in the interaction region were estimated to be $I_{FW} = 1.2 \times 10^{14}$ W/cm² and $I_{SH} = 0.5 \times 10^{14}$ W/cm², respectively. The photon ionization created ions were accelerated and guided by a weak homogeneous static electric field to be detected by a time and position sensitive detector [31] at the end of the spectrometer. The background count rate is about 40 counts per second and the count rate of the ion detector in our measurement is about 3000 counts per second (0.3 ions per laser shot). Three-dimensional momenta of the detected ions were retrieved from the measured time of flights and positions of the impacts on the detector during the offline analysis.

As compared to the nondissociative CO²⁺, here we focus on the dissociative double ionization channel (C⁺, O⁺), i.e., CO + $n\hbar\omega \rightarrow C^+ + O^+ + 2e$, for which the directional breaking of the molecule can be deduced from the emission direction of the ionic fragment of C⁺ (or O⁺) by assuming negligible

*jwu@phy.ecnu.edu.cn

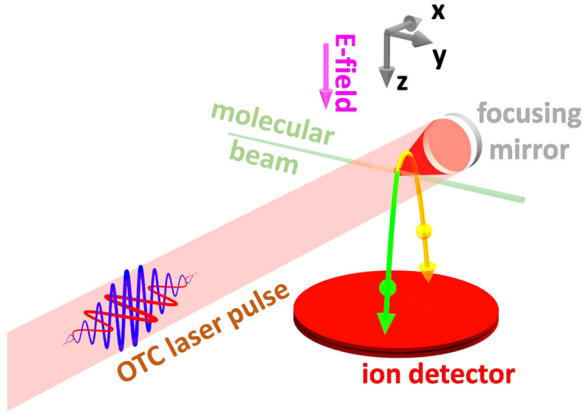


FIG. 1. Schematic diagram of the experimental apparatus.

rotation of the molecule in the ultrafast dissociative ionization process. The right event of the (C^+ , O^+) channel is selected by using the photoion-photoion coincidence method based on the momentum conservation of the detected fragments of C^+ and O^+ . Note that the C^+ (or O^+) of the dissociative single ionization channel does not satisfy the condition of momentum conservation with the O^+ (or C^+) of the (C^+ , O^+) channel if they come from two independent molecules. This coincidence measurement hence allows us to nicely distinguish the right signal of the (C^+ , O^+) channel from that of the dissociative single ionization channel.

To qualify the directional emission of C^+ from the (C^+ , O^+) channel in the polarization plane, we define the asymmetry parameter $A_{sy}(p_y, p_z, \phi_L) = [Y(p_y, p_z, \phi_L) - Y(p_y, p_z, \phi_L + \pi)] / [Y(p_y, p_z, \phi_L) + Y(p_y, p_z, \phi_L + \pi)]$, where $Y(p_y, p_z, \phi_L)$ is the measured yield of C^+ with momentum (p_y, p_z) at the laser phase ϕ_L of the OTC pulse. The asymmetry parameter is positive if C^+ is preferred to emit to $\phi_{C^+} = \arctan(p_z/p_y)$ and negative if C^+ is preferred to emit to $\phi_{C^+} + 180^\circ$ at the laser phase of ϕ_L . The electric field of the OTC pulse can be written as $\mathbf{E}(t) = E_y(t)\hat{\mathbf{e}}_y + E_z(t)\hat{\mathbf{e}}_z = f_y(t)\cos(\omega t)\hat{\mathbf{e}}_y + f_z(t)\cos(2\omega t + \phi_L)\hat{\mathbf{e}}_z$. The maximum asymmetry of the electric field vector occurs at $\phi_L = 0$ or $\phi_L = \pi$, as shown in Figs. 2(a) and 2(b), similar to the parallel polarized two-color laser field. The electric field is symmetric along the FW field, but asymmetric with respect to the SH field. By tuning the laser phase ϕ_L , the OTC field will be spatiotemporally shaped to have different strengths along various directions, allowing us to distinguish different ionization dynamics occurring within a femtosecond laser pulse.

Figures 2(c) and 2(d) display the asymmetry $A_{sy}(p_y, p_z)$ of directional emission of C^+ from the (C^+ , O^+) channel in the y - z plane at $\phi_L = 0$ and $\phi_L = \pi$, respectively. As compared to the one-dimensional steering by a parallel polarized two-color laser field, rich asymmetry structures depending on the emission direction and magnitude of the momentum of the nuclear fragments in the two-dimensional space are observed. The $A_{sy}(p_y, p_z)$ is up-down asymmetry and left-right mirrored at a given laser phase, which is reversed when the laser phase is changed by π . More interestingly, the asymmetric emission of C^+ also relies on the magnitude of the momentum of the nuclear fragments even along the same emission direction. For instance, around $\phi_{C^+} = -45^\circ$, the emitted fragments in

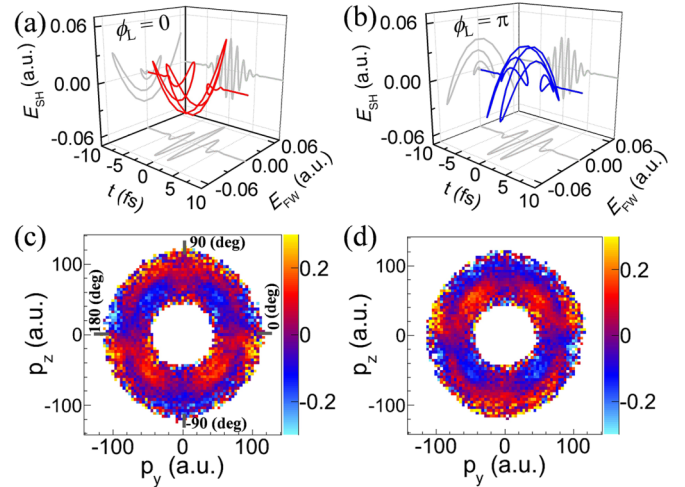


FIG. 2. (a,b) Sketch map of the spatiotemporal evolution of the electric field of the OTC laser pulse, and (c,d) measured two-dimensional asymmetry patterns of the directional emission of C^+ from the (C^+ , O^+) channel in the (p_y, p_z) plane at (a,c) $\phi_L = 0$ and (b,d) $\phi_L = \pi$, respectively.

the high- and low-momentum ranges are completely out of phase. It indicates that the phase-controlled OTC pulse allows us to steer directional breaking of the molecule along two spatial dimensions as a function of time.

To get a comprehensive view of the spatiotemporal steering of the directional bond breaking, we retrieved the contrast amplitude A_0 and phase ϕ_0 of the asymmetry as a function of the laser phase of the OTC pulse by fitting the ϕ_L -dependent asymmetry with the formula $A_{sy}(\phi_L) = Y_0 + A_0 \cos(\phi_L + \phi_0)$ for each momentum pixel (p_y, p_z) [27]. It nicely suppresses the laser phase insensitive background, i.e., the dissociative ionization induced solely by the FW or SH field. The contrast amplitude A_0 gives the strength or modulation depth of the asymmetry driven by the OTC pulse. The phase ϕ_0 (phase-of-phase) reflects the direction of the asymmetric breaking of the doubly ionized molecule, i.e., emission direction of C^+ from the (C^+ , O^+) channel, with respect to the vector of the laser phase. For instance, the preferred breaking of a CO molecule with C orientating along ϕ_{C^+} and $\phi_{C^+} + 180^\circ$ will result in a change of π of the retrieved phase ϕ_0 .

Figures 3(a) and 3(b) exhibit the amplitude A_0 and phase ϕ_0 of the ϕ_L -dependent asymmetry A_{sy} . Depending on the emission direction and kinetic energy release (KER) of the nuclear fragments, the asymmetry is distinguished into three regions as denoted in Fig. 3(a), i.e., the region A with KER between 3.0 and 6.5 eV around $\phi_{C^+} = \pm 45^\circ$ and $\pm 135^\circ$, the region B with KER between 8.0 and 13.0 eV around $\phi_{C^+} = \pm 90^\circ$, and the region C with KER between 10.0 and 13.0 eV around $\phi_{C^+} = \pm 15^\circ$ and $\pm 165^\circ$. The normalized yield of the measured (C^+ , O^+) channel as a function of KER (or the momentum) of the nuclear fragments is shown in Fig. 4(a). The fitted amplitude and phase of the asymmetry of three different regions integrated over the corresponding KERs are plotted in Figs. 3(c) and 3(d) as a function of ϕ_{C^+} . Here two one-dimensional spectra of ϕ_{C^+} integrated over different KERs for laser phase ϕ_L and $\phi_L + \pi$ are used to calculate the asymmetry, which is afterwards numerically fitted to obtain

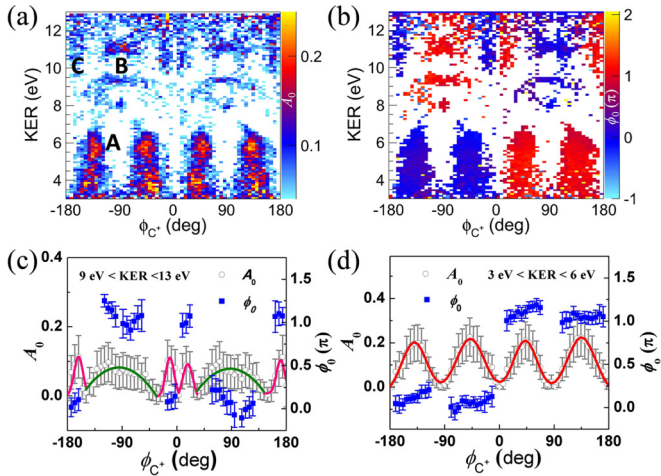


FIG. 3. Two-dimensional maps of the retrieved (a) amplitude A_0 and (b) phase ϕ_0 of the asymmetry contrast of the (C^+, O^+) channel as a function of ϕ_{C^+} and KER of the nuclear fragments. (c,d) Retrieved amplitude A_0 and phase ϕ_{A_0} as a function ϕ_{C^+} for various KER ranges. The solid curves are the fits of the ϕ_{C^+} -resolved asymmetry amplitude.

the A_0 and ϕ_0 as a function of ϕ_{C^+} in Figs. 3(c) and 3(d). No asymmetry exactly along $\phi_{C^+} = 0^\circ$ or $\pm 180^\circ$ is observed since there is no SH component along the FW field for the OTC pulse. The A_0 is mirrored by $\phi_{C^+} = 0^\circ$, but the ϕ_0 is shifted by π for CO molecule with C orientating along ϕ_{C^+} and $\phi_{C^+} + 180^\circ$. The KER- and ϕ_{C^+} -dependent asymmetry of the directional emission of C^+ indicates different double ionization dynamics steered by the spatiotemporally shaped OTC pulse.

III. DISCUSSIONS

In strong laser fields, double ionization of atoms and molecules occurs via either sequential or nonsequential processes by releasing two electrons one after the other or simultaneously. The nonsequential double ionization (NSDI) was proposed to understand the unexpected enhanced double ionization rate [32–35] and the correlated dynamics of two freed electrons of their momenta [36–39] and kinetic energies [40–42]. In general, the NSDI is preferred at modest laser

intensity assisted by the electron rescattering [32–35,41], while the sequential double ionization (SDI) dominates at high laser intensity where two electrons can be released directly by the field in the sequential manner without the requisition of rescattering. For an intense ultrashort laser pulse, SDI and NSDI may occur at different instants within the laser pulse due to the temporal evolution of the field strength. Although both the SDI and NSDI occur, the eventual observation mainly reflects the dominating process and the subordinate one is hard to identify.

Interestingly, the OTC pulse allows us to steer the electron dynamics in both time and space domains [43,44], opening the possibility to distinguish the SDI and NSDI of molecules occurring within an intense ultrashort laser pulse. Controlled by the laser phase, the instantaneous field strength of the OTC pulse evolves as a function of both time and space, i.e., the field strength varies as it points to different directions. For instance, at $\phi_L = 0$ the instantaneous field strength of the OTC pulse is estimated to be $\sim 1.7 \times 10^{14}$ W/cm² when it points to 33° or 147° , and 0.5×10^{14} W/cm² when it points to -90° . It is consistent with the dominating emission of slow C^+ to the angles of $-180^\circ < \phi_{C^+} < -120^\circ$ and $-60^\circ < \phi_{C^+} < 0^\circ$, as shown in Fig. 2(c) or region A denoted in Fig. 3(a), since CO is more likely to be ionized by a laser field pointing from C to O along the molecular axis [45,46]. Our measurements using a linearly polarized femtosecond pulse confirm that the (C^+, O^+) double ionization channel is mostly produced for molecules orientating parallel to the field direction. The high laser intensity favors the SDI of CO with molecular axis along the field direction; i.e., the first ionization-created CO^+ stretches to a large internuclear distance where the second electron is released. The Coulomb explosion of this stretched molecule results in slow nuclear fragments with KER smaller than 6 eV as shown in Fig. 3(a). Inversely proportional to the internuclear distance of the Coulomb explosion [47], the KER of the nuclear fragments has been used to determine the structure of molecules [48–54] and to reveal strong-field ionization dynamics of molecules [42]. For explosive double ionization with a Coulomb potential of $1/R$ (in atomic units), the Coulomb explosion of the stretched molecule occurs at internuclear distances between 4.5 and 9.0 a.u. for the slow fragments with KERs between 3 and 6 eV. On the other hand, the relatively weak instantaneous field pointing to -90° favors the breaking CO molecule via NSDI at short internuclear distances (2.1–3.0 a.u. for KERs between 9 and 13 eV) by simultaneously releasing two electrons within a short time interval, leading to fast C^+ emitting to 90° as shown in Fig. 2(c) [or the region B denoted in Fig. 3(a)]. Similarly, the asymmetric emission of fast C^+ in region C is mainly produced via the NSDI by a relatively weak laser field pointing close to 0° or 180° .

As shown in Fig. 4(a), the NSDI yield at high KER (9–13 eV) produced by a weak laser field is much lower than the SDI yield at low KER (3–6 eV) generated by a strong laser field. The yield ratio of the (C^+, O^+) channel between the high (9–13 eV) and low (3–6 eV) KERs is less than 28%, which agrees with previous measurements that the explosive double ionization channel is mainly accessed via the SDI [55]. As the intermediate (transition) region between the high and low KERs asymmetry between 6.5 and 8 eV is hardly observed

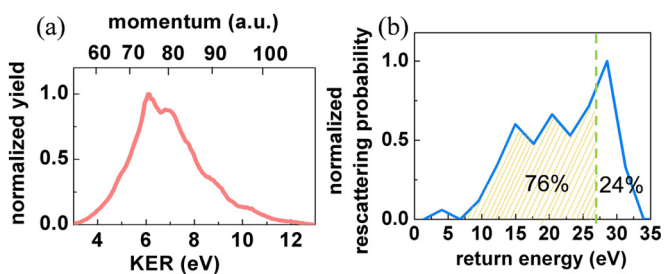


FIG. 4. (a) Normalized yield of the measured (C^+, O^+) channel as a function of KER (or momentum) of the nuclear fragments. (b) Simulated rescattering probability of the electron versus its return energy at the recolliding time. The dashed green line denotes the ionization potential of CO^+ .

as shown in Fig. 3(a). Therefore, the spatiotemporally shaped OTC laser pulse distinguishes the SDI and NSDI of CO into the directional emission of fast and slow C^+ along various directions in the polarization plane.

The NSDI can occur via either the recollision-induced excitation with subsequent ionization [56,57] or the $(e, 2e)$ process [38,41] depending on the return energy of the rescattering electron. We analyzed the trajectory of a directly emitted electron in the OTC pulse by numerically solving two-dimensional Newton's equations of the motion of the liberated electron. The electron is tunneled at an initial exit given by $(y, z) = -I_p/|\mathbf{E}(t)|^2[E_y(t), E_z(t)]$ with zero longitudinal momentum and transverse momentum distribution calculated by the ADK theory [58,59], where I_p is the single ionization potential of CO. It afterwards propagates in a modeled Coulomb potential of $V(y, z) = -1/(y^2 + z^2 + \alpha)^{1/2}$, where the soft-core parameter is set as $\alpha = 0.6$ a.u. [60]. The calculated rescattering probability of the electron as a function of the return energy at the recolliding time is displayed in Fig. 4(b). Here, we only selected the trajectory in which the electron has passed the parent ion (represented by a charge point located at the origin of the coordinates) at a distance smaller than 7 a.u. so that it potentially could lead to the double ionization following the recollision. A "recollision" distance of 5 a.u. was used in the trajectory analysis of the NSDI of argon atom [35]. We numerically confirmed that the using of recollision distances between 5 and 8 a.u. led to similar return energy spectra in our simulations. More than 10^5 trajectories of electrons emitted at different instants within the OTC pulse of different laser phases ϕ_L over 2π were launched in our calculation. As shown in Fig. 4(b), the return energy of

the rescattering electron is widely distributed between 7 and 32 eV. For the ionization potential of CO^+ at 27 eV (denoted by the dashed green line), about 24% of rescattering electrons have return energy larger than the ionization threshold of the molecular ion and may directly kick out a second electron via the $(e, 2e)$ process, while the return energy of 76% rescattering electrons is smaller than the ionization threshold. We hence expect that the NSDI in our experiment is mostly accessed via the recollision-induced excitation with subsequent ionization.

IV. CONCLUSION

In summary, we report experimental observation of two-dimensional directional breaking of a doubly ionized CO molecule by controlling the phase of an intense OTC laser pulse. The energy- and angle-resolved directional emission of the nuclear fragments driven by the spatiotemporally shaped OTC pulse allows us to get deep insights of the complicated strong-field dynamics of molecules. In particular, the SDI and NSDI occurring within an intense laser pulse could be illustratively visualized by the retrieved amplitude and phase of the asymmetry contrast as a function of the laser phase.

ACKNOWLEDGMENTS

We thank F. He, J. Wang, and Z. Li for fruitful discussions. This work is supported by the National Natural Science Foundation of China (Grants No. 11425416, No. 61690224, and No. 11621404), the Shanghai Sailing Program (Grant No. 16YF1402900), and the Program of Introducing Talents of Discipline to Universities (Grant No. B12024).

-
- [1] A. Assion, T. Baumert, M. Bergt, T. Brixner, B. Kiefer, V. Seyfried, M. Strehle, and G. Gerber, *Science* **282**, 919 (1998).
 - [2] M. Shapiro and P. Brumer, *Rep. Prog. Phys.* **66**, 859 (2003).
 - [3] M. F. Kling, Ch. Siedschlag, A. J. Verhoef, J. I. Khan, M. Schultze, Th. Uphues, Y. Ni, M. Uiberacker, M. Drescher, F. Krausz, and M. J. J. Vrakking, *Science* **312**, 246 (2006).
 - [4] M. Kremer, B. Fischer, B. Feuerstein, V. L. B. de Jesus, V. Sharma, C. Hofrichter, A. Rudenko, U. Thumm, C. D. Schröter, R. Moshhammer, and J. Ullrich, *Phys. Rev. Lett.* **103**, 213003 (2009).
 - [5] B. Fischer, M. Kremer, T. Pfeifer, B. Feuerstein, V. Sharma, U. Thumm, C. D. Schröter, R. Moshhammer, and J. Ullrich, *Phys. Rev. Lett.* **105**, 223001 (2010).
 - [6] J. McKenna, F. Anis, A. M. Sayler, B. Gaire, N. G. Johnson, E. Parke, K. D. Carnes, B. D. Esry, and I. Ben-Itzhak, *Phys. Rev. A* **85**, 023405 (2012).
 - [7] H. Xu, T. Y. Xu, F. He, D. Kielpinski, R. T. Sang, and I. V. Litvinyuk, *Phys. Rev. A* **89**, 041403(R) (2014).
 - [8] E. Charron, A. Giusti-Suzor, and F. H. Mies, *Phys. Rev. Lett.* **71**, 692 (1993).
 - [9] B. Sheehy, B. Walker, and L. F. DiMauro, *Phys. Rev. Lett.* **74**, 4799 (1995).
 - [10] H. Ohmura, N. Saito, and M. Tachiya, *Phys. Rev. Lett.* **96**, 173001 (2006).
 - [11] D. Ray, F. He, S. De, W. Cao, H. Mashiko, P. Ranitovic, K. P. Singh, I. Znakovskaya, U. Thumm, G. G. Paulus, M. F. Kling, I. V. Litvinyuk, and C. L. Cocke, *Phys. Rev. Lett.* **103**, 223201 (2009).
 - [12] K. J. Betsch, D. W. Pinkham, and R. R. Jones, *Phys. Rev. Lett.* **105**, 223002 (2010).
 - [13] J. Wu, A. Vredenburg, L. Ph. H. Schmidt, T. Jahnke, A. Czasch, and R. Dörner, *Phys. Rev. A* **87**, 023406 (2013).
 - [14] Q. Song, X. Gong, Q. Ji, K. Lin, H. Pan, J. Ding, H. Zeng, and J. Wu, *J. Phys. B: At., Mol. Opt. Phys.* **48**, 094007 (2015).
 - [15] V. Wanie, H. Ibrahim, S. Beaulieu, N. Thiré, B. E. Schmidt, Y. Deng, A. S. Alnaser, I. V. Litvinyuk, X. Tong, and F. Légaré, *J. Phys. B: At., Mol. Opt. Phys.* **49**, 025601 (2016).
 - [16] A. D. Bandrauk, S. Chelkowski, and H. S. Nguyen, *Int. J. Quantum Chem.* **100**, 834 (2004).
 - [17] X. M. Tong and C. D. Lin, *Phys. Rev. Lett.* **98**, 123002 (2007).
 - [18] V. Roudnev and B. D. Esry, *Phys. Rev. Lett.* **99**, 220406 (2007).
 - [19] F. Kelkensberg, G. Sansone, M. Y. Ivanov, and M. Vrakking, *Phys. Chem. Chem. Phys.* **13**, 8647 (2011).
 - [20] J. Wu, M. Magrakvelidze, L. Ph. H. Schmidt, M. Kunitski, T. Pfeifer, M. Schöffler, M. Pitzer, M. Richter, S. Voss, H. Sann, H. Kim, J. Lower, T. Jahnke, A. Czasch, U. Thumm, and R. Dörner, *Nat. Commun.* **4**, 2177 (2013).
 - [21] X. M. Tong, Z. X. Zhao, and C. D. Lin, *Phys. Rev. A* **66**, 033402 (2002).

- [22] O. I. Tolstikhin, T. Morishita, and L. B. Madsen, *Phys. Rev. A* **84**, 053423 (2011).
- [23] J. Muth-Böhm, A. Becker, and F. H. M. Faisal, *Phys. Rev. Lett.* **85**, 2280 (2000).
- [24] L. Holmegaard, J. L. Hansen, L. Kalhøj, S. L. Kragh, H. Stapelfeldt, F. Filsinger, J. Küpper, G. Meijer, D. Dimitrovski, M. Abu-samha, C. P. J. Martiny, and L. B. Madsen, *Nat. Phys.* **6**, 428 (2010).
- [25] D. Dimitrovski, M. Abu-samha, L. B. Madsen, F. Filsinger, G. Meijer, J. Küpper, L. Holmegaard, L. Kalhøj, J. H. Nielsen, and H. Stapelfeldt, *Phys. Rev. A* **83**, 023405 (2011).
- [26] Q. Song, Z. Li, S. Cui, P. Lu, X. Gong, Q. Ji, K. Lin, W. Zhang, J. Ma, H. Pan, J. Ding, M. F. Kling, H. Zeng, F. He, and J. Wu, *Phys. Rev. A* **94**, 053419 (2016).
- [27] X. Gong, P. He, Q. Song, Q. Ji, H. Pan, J. Ding, F. He, H. Zeng, and J. Wu, *Phys. Rev. Lett.* **113**, 203001 (2014).
- [28] K. Lin, X. Gong, Q. Song, Q. Ji, W. Zhang, J. Ma, P. Lu, H. Pan, J. Ding, H. Zeng, and J. Wu, *J. Phys. B: At., Mol. Opt. Phys.* **49**, 025603 (2016).
- [29] R. Dörner, V. Mergel, O. Jagutzki, L. Spielberger, J. Ullrich, R. Moshhammer, and H. Schmidt-Böcking, *Phys. Rep.* **330**, 95 (2000).
- [30] J. Ullrich, R. Moshhammer, A. Dorn, R. Dörner, L. Ph. H. Schmidt, and H. Schmidt-Böcking, *Rep. Prog. Phys.* **66**, 1463 (2003).
- [31] O. Jagutzki, A. Cerezo, A. Czasch, R. Dörner, M. Hattabaß, M. Huang, V. Mergel, U. Spillmann, K. Ullmann-Pfleger, Th. Weber, H. S. Böcking, and G. D.W. Smith, *IEEE Trans. Nucl. Sci.* **49**, 2477 (2002).
- [32] C. Guo, M. Li, J. P. Nibarger, and G. N. Gibson, *Phys. Rev. A* **58**, R4271(R) (1998).
- [33] C. Guo and G. N. Gibson, *Phys. Rev. A* **63**, 040701(R) (2001).
- [34] C. A. Mancuso, K. M. Dorney, D. D. Hickstein, J. L. Chaloupka, J. L. Ellis, F. J. Dollar, R. Knut, P. Grychtol, D. Zusin, C. Gentry, M. Gopalakrishnan, H. C. Kapteyn, and M. M. Murnane, *Phys. Rev. Lett.* **117**, 133201 (2016).
- [35] S. Eckart, M. Richter, M. Kunitski, A. Hartung, J. Rist, K. Henrichs, N. Schlott, H. Kang, T. Bauer, H. Sann, L. Ph. H. Schmidt, M. Schöffler, T. Jahnke, and R. Dörner, *Phys. Rev. Lett.* **117**, 133202 (2016).
- [36] Y. Zhou, Q. Liao, Q. Zhang, W. Hong, and P. Lu, *Opt. Express* **18**, 632 (2010).
- [37] Y. Zhou, C. Huang, A. Tong, Q. Liao, and P. Lu, *Opt. Express* **19**, 2301 (2011).
- [38] B. Bergues, M. Kübel, N. G. Johnson, B. Fischer, N. Camus, K. J. Betsch, O. Herrwerth, A. Senfleben, A. Max Saylor, T. Rathje, T. Pfeifer, I. Ben-Itzhak, R. R. Jones, G. G. Paulus, F. Krausz, R. Moshhammer, J. Ullrich, and M. F. Kling, *Nat. Commun.* **3**, 813 (2012).
- [39] L. Zhang, X. Xie, S. Roither, Y. Zhou, P. Lu, D. Kartashov, M. Schöffler, D. Shafir, P. B. Corkum, A. Baltuška, A. Staudte, and M. Kitzler, *Phys. Rev. Lett.* **112**, 193002 (2014).
- [40] Y. Liu, X. Liu, Y. Deng, C. Wu, H. Jiang, and Q. Gong, *Phys. Rev. Lett.* **106**, 073004 (2011).
- [41] X. Xie, K. Doblhoff-Dier, S. Roither, M. S. Schöffler, D. Kartashov, H. Xu, T. Rathje, G. G. Paulus, A. Baltuška, S. Gräfe, and M. Kitzler, *Phys. Rev. Lett.* **109**, 243001 (2012).
- [42] X. Gong, Q. Song, Q. Ji, K. Lin, H. Pan, J. Ding, H. Zeng, and J. Wu, *Phys. Rev. Lett.* **114**, 163001 (2015).
- [43] M. Kitzler and M. Lezius, *Phys. Rev. Lett.* **95**, 253001 (2005).
- [44] Z. Yuan, D. Ye, Q. Xia, J. Liu, and L. Fu, *Phys. Rev. A* **91**, 063417 (2015).
- [45] H. Li, D. Ray, S. De, I. Znakovskaya, W. Cao, G. Laurent, Z. Wang, M. F. Kling, A. T. Le, and C. L. Cocke, *Phys. Rev. A* **84**, 043429 (2011).
- [46] J. Wu, L. Ph. H. Schmidt, M. Kunitski, M. Meckel, S. Voss, H. Sann, H. Kim, T. Jahnke, A. Czasch, and R. Dörner, *Phys. Rev. Lett.* **108**, 183001 (2012).
- [47] Z. Vager, R. Naaman, and E. P. Kanter, *Science* **244**, 426 (1989).
- [48] Y. Muramatsu, K. Ueda, N. Saito, H. Chiba, M. Lavollée, A. Czasch, T. Weber, O. Jagutzki, H. Schmidt-Böcking, R. Moshhammer, U. Becker, K. Kubozuka, and I. Koyano, *Phys. Rev. Lett.* **88**, 133002 (2002).
- [49] F. Légaré, K. F. Lee, I. V. Litvinyuk, P. W. Dooley, S. S. Wesolowski, P. R. Bunker, P. Dombi, F. Krausz, A. D. Bandrauk, D. M. Villeneuve, and P. B. Corkum, *Phys. Rev. A* **71**, 013415 (2005).
- [50] K. Zhao and W. T. Hill III, *Phys. Rev. A* **71**, 013412 (2005).
- [51] J. Gagnon, K. F. Lee, D. M. Rayner, P. B. Corkum, and V. R. Bhardwaj, *J. Phys. B: At., Mol. Opt. Phys.* **41**, 215104 (2008).
- [52] A. Hishikawa, H. Hasegawa, and K. Yamanouchi, *Chem. Phys. Lett.* **388**, 1 (2004).
- [53] J. P. Brichta, S. J. Walker, R. Helsten, and J. H. Sanderson, *J. Phys. B: At., Mol. Opt. Phys.* **40**, 117 (2007).
- [54] X. Gong, M. Kunitski, L. Ph. H. Schmidt, T. Jahnke, A. Czasch, R. Dörner, and J. Wu, *Phys. Rev. A* **88**, 013422 (2013).
- [55] C. Guo, *Phys. Rev. A* **73**, 041401(R) (2006).
- [56] R. Kopold, W. Becker, H. Rottke, and W. Sandner, *Phys. Rev. Lett.* **85**, 3781 (2000).
- [57] B. Feuerstein, R. Moshhammer, D. Fischer, A. Dorn, C. D. Schröter, J. Deipenwisch, J. R. Crespo Lopez-Urrutia, C. Höhr, P. Neumayer, J. Ullrich, H. Rottke, C. Trumpf, M. Wittmann, G. Korn, and W. Sandner, *Phys. Rev. Lett.* **87**, 043003 (2001).
- [58] L. D. Landau and E. M. Lifshitz, *Quantum Mechanics* (Pergamon, Oxford, 1977).
- [59] M.-M. Liu, M. Li, C. Wu, Q. Gong, A. Staudte, and Y. Liu, *Phys. Rev. Lett.* **116**, 163004 (2016).
- [60] P.-L. He, N. Takemoto, and F. He, *Phys. Rev. A* **91**, 063413 (2015).